A Novel HIF-2α/ARNT Signaling Pathway Protects Against Microvascular Dysfunction and heart failure After Myocardial Infarction

Karim Ullah[1&], Lizhuo Ai[1,7 &], Yan Li[2], Lifeng Liu[1], Qin Zhang[1], Kaichao Pan[1], Zainab Humayun[1], Albert Sitikov[1], Qiaozhu Su [3], Qiong zhao[4], Willard Sharp[5], Yun Fang[6], David Wu[6], James K. Liao[8] and Rongxue Wu[1*]

[1]Section of Cardiology, Department of Medicine, Biological sciences Division. University of Chicago, Chicago, IL; USA
[2] Department of Human Genetics, University of Chicago, Chicago, IL, USA.
[3] Institute for Global Food Security, School of Biological Sciences, Queen's University Belfast, United Kingdom
[4] Division of Cardiology, Department of Medicine, Inova Heart and Vascular Institute, USA
[5] Emergency Medicine; Department of Medicine, University of Chicago, Chicago, IL.
[6]Section of Pulmonary and Critical Care, Department of Medicine, University of Chicago
[7] The Smidt Heart Institute, Cedars-Sinai Medical Center, Los Angeles, USA
[8] Department of Medicine, University of Arizona. USA

[&] Equal contributions
*Corresponding author: Rongxue Wu, rwu3@uchiago.edu

Running title:
HIF-2α/ARNT Signaling Protects Microvascular Dysfunction

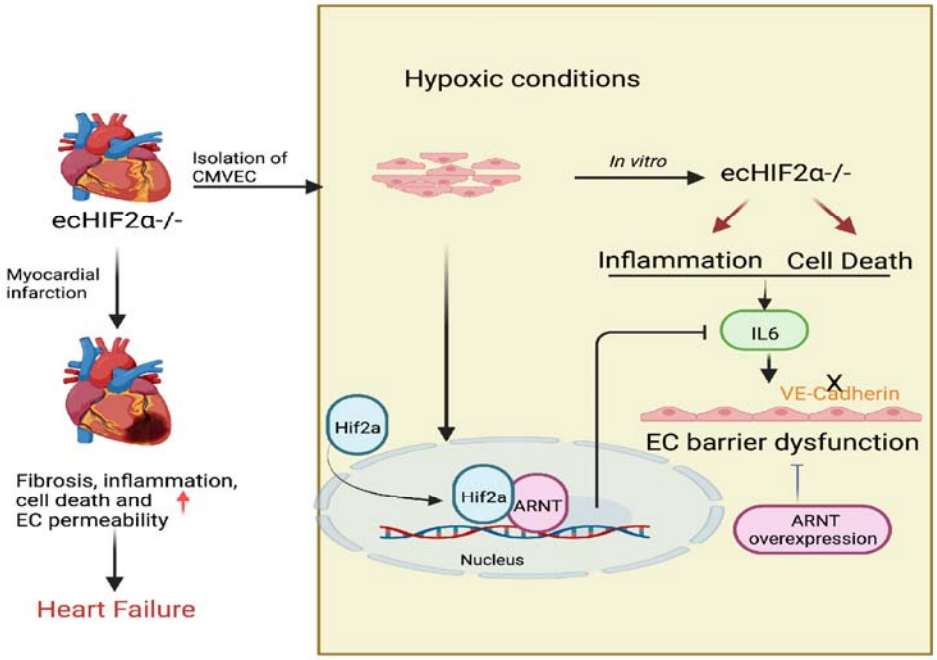

Diagram of the role of HF2a/ARNT in the cardiac MI.

ABSTRACT

Rationale
Cardiac microvascular leakage and inflammation are triggered during myocardial infarction (MI) and contribute to heart failure. Hypoxia-inducible factor 2α (*Hif2α*) is highly expressed in endothelial cells (ECs) and rapidly activated by myocardial ischemia, but whether it has a role in endothelial barrier function during MI is unclear.

Objective
To test our hypothesis that the expression of Hif2α and its binding partner aryl hydrocarbon nuclear translocator (ARNT) in ECs regulate cardiac microvascular permeability in infarcted hearts.

Methods and Results
Experiments were conducted with mice carrying an inducible EC-specific *Hif2α*-knockout (*ecHif2α*$^{-/-}$) mutation, with mouse cardiac microvascular endothelial cells (CMVECs) isolated from the hearts of *ecHif2α*$^{-/-}$ mice after the mutation was induced, and with human CMVECs and umbilical-vein endothelial cells transfected with *ecHif2α* siRNA. After MI induction, echocardiographic assessments of cardiac function were significantly lower, while measures of cardiac microvascular leakage (Evans blue assay), plasma IL6 levels, and cardiac neutrophil accumulation and fibrosis (histology) were significantly greater, in *ecHif2α*$^{-/-}$ mice than in control mice, and RNA-sequencing analysis of heart tissues from both groups indicated that the expression of genes involved in vascular permeability and collagen synthesis was enriched in *ecHif2α*$^{-/-}$ hearts. In cultured ECs, ec*Hif2α* deficiency was associated with declines in endothelial barrier function (electrical cell impedance assay) and the reduced abundance of tight-junction proteins, as well as an increase in the expression of inflammatory markers, all of which were largely reversed by the overexpression of ARNT. We also found that ARNT, but not Hif2α, binds directly to the IL6 promoter and suppresses IL6 expression.

Conclusions
EC-specific deficiencies in Hif2α expression significantly increase cardiac microvascular permeability, promote inflammation, and reduce cardiac function in infarcted mouse hearts, and ARNT overexpression can reverse the upregulation of inflammatory genes and restore endothelial-barrier function in *Hif2α*-deficient ECs.

GRAPHIC ABSTRACT: A graphic abstract is available for this article.

Keywords: myocardial infarction, hypoxia, mice, microvascular barrier function, inflammation, cardiac fibrosis. ARNT, HIF1α pathway, *Hif2α*.

Introduction

Despite many therapeutic advancements, acute myocardial infarction (MI) remains the leading cause of death in western countries[1]. The ischemia caused by an intracoronary thrombus leads to profound hypoxia, inflammation, and edema[2], and although many organs can tolerate mild to moderate edema, even small increases in interstitial fluid volume can significantly compromise cardiac function[3]. The fundamental cause of edema is an increase in vascular permeability, and some evidence suggests that cardiac function can be improved via the administration of vascular-leakage blockers, which inhibit both cardiac microvascular endothelial cell (CMVEC) hyperpermeability and the infiltration of circulating neutrophils[4]. Nevertheless, the mechanisms that regulate cardiac microvascular permeability have rarely been investigated as potential targets for the treatment of ischemic myocardial disease.

The cellular response to hypoxia leads to the stabilization of Hypoxia-inducible Factors (HIFs), including Hif1α and Hif2α, (HIF1A and HIF2A in humans), which form heterodimeric complexes with aryl hydrocarbon receptor nuclear translocator (ARNT) to activate hypoxia-inducible genes[5-8]. Hif1α and Hif2α have been linked to several physiological and pathological processes that have a role in heart disease, but the two isoforms appear to function independently and in a cell-type–specific manner. Hif1α is ubiquitously expressed in all cell types and is known to have a cardioprotective role during ischemic preconditioning[9,10, 11], whereas *Hif2α* is highly expressed in endothelial cells (ECs)[12], and its role in myocardial disease appears to be highly variable. For example, although the inhibition of *Hif2α* reversed right heart failure and pulmonary arterial hypertension in rodents[13], the cardiomyocyte-specific deletion of *Hif2α* (but not *HIF1α*) increased infarct sizes in a mouse model of ischemia-reperfusion injury[5].

Homozygous deletions of *Hif2α* are lethal during embryonic development[14-16], but mice with EC-specific deficiencies in *Hif2α* survive with a variety of aberrant phenotypes, including elevations in vessel permeability[14,17]. Thus, we generated a line of mice carrying an inducible, EC-specific, *Hif2α*-knockout (*ecHif2α*$^{-/-}$) mutation to investigate the role *Hif2α* in cardiac microvascular barrier function after experimentally induced MI. The ec*Hif2α* deficiency was associated with a significant increase in cardiac microvascular permeability in infarcted hearts, as well as disruptions in endothelial barrier activity and elevated IL6 expression in cultured ECs, and the changes observed in our in-vitro studies were largely reversed by the overexpression of ARNT. Collectively, our results have identified a novel mechanism by which Hif2α and ARNT regulate cardiac vascular function and inflammation in response to ischemic cardiac injury.

Methods

Data Availability

All data that support the findings of this study are available from the corresponding author upon request. For a detailed description of all methods and materials used, please refer to the Supplemental Methods and Major Resources Table in the Supplemental Materials.

Following left anterior descending coronary artery ligation-induced myocardial infarction, mice were randomly assigned accordingly to one of four groups: (1) sham-operated control, (2) sham-operated ec*Hif2α*$^{-/-}$, (3) control MI, and (4) ec*Hif2α*$^{-/-}$ MI. Any mice that did not survive the operation were not included in the analysis of the study. To ensure unbiased analysis, all echocardiographic, cellular, and molecular assessments were conducted in a blinded manner.

Results

Endothelial *Hif2α* deletion impairs endothelial barrier function after MI.

Our breeding program began with *Hif2α*$^{flox/flox}$ mice (C57BL/6 background; The Jackson Laboratory) and transgenic mice expressing tamoxifen-inducible Cre recombinase (CreERT2) under the control of the EC-specific VE-Cadherin promoter (Fig. 1A) [18]. After two generations, the *Hif2α*$^{flox/flox+Cre}$ offspring were fed tamoxifen chow for two weeks to generate the experimental *ecHif2α*$^{-/-}$ mice, and control assessments were conducted with *Hif2α*$^{flox/flox}$ mice fed tamoxifen chow and with *Hif2α*$^{flox/flox+Cre}$ mice fed normal (tamoxifen-free) chow. (Supplemental Fig.1A-B). Mouse genotypes were verified via PCR (Fig. 1B), and the efficiency of *Hif2α* knockout induction was confirmed via analysis of *Hif2α* mRNA abundance in primary ECs isolated from *Hif2α*$^{flox/flox}$ mice fed tamoxifen chow and *ecHif2α*$^{-/-}$ mice upon completion of the feeding protocol (Fig. 1C). The mice were phenotypically normal with no significant changes in body weight, heart weight, blood pressure, or cardiac function (Supplemental Fig. 2-4). As neither control group showed any noticeable difference at baseline, we opted to use only *Hif2α*$^{flox/flox}$ mice as controls to reduce the usage of animals.

MI was induced in *ecHif2α*$^{-/-}$ mice and in Control mice via ligation of the left anterior descending (LAD) coronary artery, and another group of *ecHif2α*$^{-/-}$ mice (the Sham group) underwent all surgical procedures for MI induction except coronary artery ligation (Supplemental Fig. 5). Evans Blue dye was injected into the tail veins of mice 12 hours after MI induction or Sham surgery, and hearts were harvested 30 minutes later after Evans blue injection. Measurements of Evans blue extravasation were significantly greater in *ecHif2α*$^{-/-}$ hearts than in the hearts of Control or Sham mice (Fig. 1D), but significant differences were not observed between the two groups for organs under normoxia condition (Supplemental Fig. 6). Furthermore, when cells were cultured under hypoxic conditions, VE-cadherin (Fig. 1E) was significantly less abundant in CMVEC isolated from *ecHif2α*$^{-/-}$ hearts than in Control ECs (Fig. 1E) and in human microvascular endothelial cells (hMVECs) (Fig. 1F-G) as well as HUVEC (Supplemental Fig. 7) transfected with *Hif2α* siRNA than in control siRNA transfected cells. In addition, the expression of Zonula occludens-1 (ZO-1), a tight junction protein that plays a critical role in endothelial barrier function, was also reduced in hMVECs with *Hif2α* deficiency under hypoxia condition. (Supplemental Fig. 8). *In ex vivo*, measurements of transendothelial resistance (TER) were also significantly lower in monolayers of mouse cardiac microvascular endothelial cells (mCMVECs) from *ecHif2α*$^{-/-}$ mice than in Control mCMVEC monolayers (Fig. 1H-I) under hypoxia condition induced by DMOG (dimethyloxalylglycine). The above results indicate that endothelial-specific loss of *Hif2α* expression increased vascular permeability in infarcted hearts, reduced junctional protein expression in cultured ECs, and impaired barrier function in mCMVEC monolayers. Notably, serum levels of the inflammatory protein IL6, but not TNF*α* or IL1b (Supplemental Fig. 9) were significantly higher in *ecHif2α*$^{-/-}$ mice than in Control mice 12 hours after MI induction (Fig. 1J), suggests that *ecHif2α* expression may also have a systemic role in the inflammatory response to cardiac injury, which is related to IL6.

Endothelial *Hif2α* deletion exacerbates cardiac dysfunction and fibrosis in infarcted hearts.

Cardiac function was evaluated by echocardiography (Fig. 2A) before MI induction (baseline) and seven and 28 days afterward. Baseline measurements of left-ventricular ejection fraction (EF, Fig. 2B), fractional shortening (FS, Fig. 2C), and cardiac output (Fig. 2D) in *ecHif2α*$^{-/-}$ and Control mice were similar, but EF was significantly lower on Day 7, and all three parameters were significantly lower on Day 28, in *ecHif2α*$^{-/-}$ mice. Furthermore, assessments in hearts collected on Day 28 indicated that the *ecHif2α* deletion was associated with notable increases in heart size (Fig. 2E), myocardial fibrosis, and inflammatory cell infiltration (Fig. 2F), and with significant increases in the expression of *Col13a1* (Fig. 2G) and *Lox3* (Supplemental Fig. 10A), as well as the heart failure markers *BNP* (Fig. 2I) and *NPR3* (Fig. 2H). Survival rates were also

significantly lower in *ecHif2α*$^{-/-}$ mice than in Control mice (Fig. 2J). Thus, *ecHif2α* expression appears to have a crucial cardioprotective role in response to ischemic injury.

Endothelial *Hif2α* deletion alters the expression of endothelial permeability related genes after MI.

Bulk RNA-seq analysis of heart tissues collected 28 Days after MI induction or Sham surgery identified 130 genes that were differentially expressed in the infarcted hearts of *ecHif2α*$^{-/-}$ and Control mice (Fig. 3A and Table 1.1). Eighty-six of the differentially expressed genes (DEGs) were upregulated in *ecHif2α*$^{-/-}$ hearts, including many genes that are known to increase vascular permeability and fibrosis, while the remaining 44 downregulated DEGs included many of those that promote vascular barrier function (Fig. 3B-C). These observations were supported by pathway enrichment analysis, which indicated that genes involved in vascular permeability, collagen-containing extracellular matrix production, and cell-matrix adhesion were significantly enriched in the DEGs (Fig. 3D). Additionally, measurements of mRNA abundance confirmed that regulators of vessel-permeability and collagen synthesis (*plvap* and *P3h2* respectively) were more highly expressed, while the expression of known regulators of endothelial barrier function (e.g., such as *cdh-5*, *tjp-1*, and *angpt-2*) was significantly lower, in *ecHif2α*$^{-/-}$ than in Control hearts after MI (Fig. 3E-G and Supplemental Fig**.** 10B,C). Notably, the *ecHif2α* deletion was also associated with a significant increase in mRNA levels for the inflammatory IL6 and VCAM-1 (Fig 3H, I) , while ICAM, and e-selectin expression tended to be greater (though not significantly) in infarcted *ecHif2α*$^{-/-}$ hearts than infarcted Control hearts (Supplemental Fig. 11) which is consistent with our observation that the MI-induced cardiac infiltration of inflammatory cells was greater in *ecHif2α*$^{-/-}$ mice than in Control mice.

***Hif2α* deficiency impairs angiogenetic activity and promotes apoptosis in cultured ECs.**

Because vascular permeability and angiogenesis are closely linked[19, 20], we investigated whether the aberrations in vascular barrier function associated with *ecHif2α* deletion were accompanied by changes in the angiogenic activity of ECs. The results from tube formation assays in HUVECs that had been transfected with siHif2α or control siRNA (Fig. 4A) indicated that nodes and junctions were significantly less common in networks of *Hif2α*-deficient HUVECs than in Control HUVEC networks when the cells were cultured under low oxygen levels, and that *Hif2α* deficiency was associated with declines in mesh formation and total tube length under both normoxic and hypoxic conditions (Fig. 4B-E). Furthermore, although assessments of cellular health (Fig. 4F) and apoptosis (Fig. 4G-H) did not differ significantly between *Hif2α*-deficient and Control HUVECs when the cells were cultured under normal oxygen levels, the *Hif2α*-deficiency was associated with greater evidence of early-stage apoptosis under hypoxic conditions. Collectively, these data suggest that the *ecHif2α* deletion likely impairs vascular growth and EC survival in oxygen-poor microenvironments, such as infarcted myocardium.

Overexpression of ARNT restores endothelial barrier integrity in *Hif2α*-deficient ECs.

Because *Hif2α* functions as a heterodimer with ARNT,[8] we investigated whether overexpressing ARNT could compensate for the deleterious effects associated with the loss of ec*Hif2α* activity. Experiments were conducted in HMVECs and HUVECs that had been transfected with siHif2α or a control (scrambled) siRNA and co-transfected with vectors coding for wild-type ARNT (ARNT^{WT}) or an ARNT mutant (ARNT^{mut}, containing a point mutation that prevents ARNT-mediated transcription by blocking phosphorylation of the wild-type S77 residue)[21]. ARNT overexpression displayed nuclear localization as expected (Supplemental Fig. 12). ARNT^{WT}, but not ARNT^{mut}, overexpression reduced hypoxia-induced apoptosis (Fig. 5A) and restored VE-cadherin expression to normal levels in si*Hif2α*-transfected HMVECs (Fig. 5B), and whereas ECIS assays demonstrated that *Hif2α* inactivation reduced barrier function in HUVEC monolayers not at normaxial condition, but at hypoxia condition induced by

dimethyloxalylglycine (DMOG), which is a compound that is commonly used to mimic hypoxia in cell culture experiments. (Fig. 5C-D). Measurements of minimum resistance, which occurred 40 minutes after hyperpermeability was induced via treatment with thrombin, were much greater in HMVEC monolayers when the cells were transfected with both si*Hif2α* and $ARNT^{WT}$ than with si*Hif2α* alone or si*Hif2α* and $ARNT^{mut}$ (Fig. 5E). Thus, $ARNT^{WT}$ overexpression appears to reverse the decline in both EC survival and endothelial barrier function associated with *Hif2α* deficiency.

ARNT overexpression reverses IL6 upregulation in *Hif2α*-deficient ECs by directly binding to IL6 promoter.

$ARNT^{WT}$ overexpression was also associated with declines in the abundance of IL6 protein and TNFα mRNA, in siHif2α-transfected HMVECs (Fig. 6A and Supplemental Fig. 13), and when human aortic endothelial cells (HAECs) were cultured under hypoxic conditions, the abundance of IL6, ICAM, VCAM-1, and TNFα mRNA (Fig. 6B), as well as IL6 protein levels (Fig. 6C-F) were lower in HAECs transfected with siHif2α and $ARNT^{WT}$ than in HAECs transfected with siHif2α alone. Thus, we began to investigate the mechanism by which ARNT appears to antagonize the increase in inflammation associated with siHif2α inactivation by conducting experiments in HEK293 cells carrying an IL6-luciferase promoter-reporter construct. Luciferase activity declined significantly when the cells were incubated under hypoxic conditions (Fig. 7A-B) and increased significantly when the cells were transfected with si*Hif2α*; however, when the cells were transfected with siHif2α and $ARNT^{WT}$, measurements of luciferase activity were similar to those in cells transfected with a Control (scrambled) siRNA and significantly lower than in siHif2α-transfected cells or in cells co-transfected with siHIF2α and $ARNT^{mut}$ (Fig. 7C). Furthermore, the results from ChIP-qPCR analysis indicated that ARNT, but not Hif2α, binds directly with the IL6 promoter (7D-E). Thus, in the absence of Hif2α, overexpression of ARNT may preserve endothelial barrier function, at least in part, by suppressing both IL6 expression and inflammation.

Discussion

Although HIF1α is generally considered to be the primary mediator of the hypoxic response pathway[22-24], *Hif2α* has a protective role in kidney ischemia and myocardial ischemia-reperfusion injury[25,5].

Here, we show that the EC-specific loss of *Hif2α* alters the expression of genes (e.g., CDH5 and PLVAP[26, 27]) that directly or indirectly control vascular permeability, which impairs endothelial barrier function, promotes inflammation, and worsens both cardiac performance and fibrosis in infarcted mouse hearts. We also demonstrated that the angiogenic activity and hypoxic resistance of cultured ECs declined in response to siRNA-mediated Hif2α inactivation, that the upregulated expression of inflammatory genes and endothelial-barrier dysfunction observed in *Hif2α*-deficient ECs could be mitigated via the overexpression of ARNT, and that ARNT, but not Hif2α, bound directly to the IL6 promoter and suppressed IL6 expression. Collectively, our observations are consistent with previous reports linking microvascular dysfunction to a variety of pathological processes, including inflammation, apoptosis[3, 28,29-31], and impaired angiogenesis[32, 33], and suggest that Hif2α/ARNT heterodimers are crucial regulators of endothelial barrier integrity and function in ischemic hearts.

Numerous studies have shown that HIF activation can suppress inflammation[34-36], and that inflammation increases vascular permeability by destabilizing endothelial junctional proteins[37-39,40]. IL6 is a prominent regulator of both inflammation[41] and vascular permeability[42], and although the role of IL6 induction in the ECs of infarcted hearts has yet to be thoroughly characterized, inhibition of IL6 attenuates inflammation and prevents endothelial barrier disruption in retinal ECs[43]. Notably, Hif2α-dependent reductions in IL6 expression have also been observed in inflammatory macrophages[44], but another report suggests that Hif2α

upregulates IL6 expression in cardiomyocytes by binding directly to hypoxia response elements in the IL6 promoter[45] However, in our study, it was found that Hif2α does not directly bind to the IL6 promoter, but rather indirectly through ANRT. This finding helps to clarify the complex relationship between Hif2α and IL6 expression in different cellular contexts. Thus, the role of Hif2α during inflammation[44, 46-48] appears to be strongly dependent on cell type. Furthermore, whereas mice carrying a noninducible EC-specific *Hif2α* knockout mutation develop normally[14], the EC-specific deletion of ARNT leads to liver necrosis, cardiac hemorrhage, and death in utero[49], while ARNT deficiencies in adipose cells protect mice from age and diet-induced glucose intolerance[50], so whether the Hif2α/ARNT axis may have a role in these or other pathological processes could be investigated in future studies.

In conclusion, the results from our investigation demonstrate that EC-specific deficiencies in Hif2α expression significantly increase cardiac microvascular permeability, promote inflammation, and reduce cardiac function in infarcted mouse hearts, and that ARNT overexpression can reverse the upregulation of inflammatory genes and restore endothelial-barrier function in *Hif2α*-deficient ECs. Importantly, we identify a novel mechanism by which ARNT directly inhibits IL6 expression induced by HIF2α deletion via DNA binding to the IL6 promoter region. Collectively, these findings suggest that strategies for targeting ecHif2α expression may have important clinical implications for the management of cardiac edema in patients with heart disease.

Figure Legend

Figure 1: Endothelial *Hif2α* Deletion Impairs Barrier Function in MI . (A) Schematic breeding strategy to generate endothelial cells specific inducible *Hif2α* knockout mice. *Hif2α*$^{flox/flox}$ mice were crossed with Cre-recombinase expressing mice under the control of VE-cadherin promoter. *Hif2α*$^{flox/flox+CRE}$ and *Hif2α*$^{+/+\ +CRE}$, *Hif2α*$^{flox/flox}$ mice were grouped and fed with or without tamoxifen containing food for two weeks to induce CRE recombinase activity. After two weeks, the mice underwent experimental protocol. (B) Genotyping was determined by PCR. (C) *Hif2α* mRNA expression analysis by RT-PCR confirmed the deletion of *Hif2α* gene. (D-E). Endothelial specific *Hif2α* deletion increases the permeability of heart. (D) Quantification of Evans blue dye extravasation after 24h of MI. Control vs *Hif2α*$^{-/-}$ MI mice p= 0.003, n=3. (F) Immunofluorescence staining of VE-Cadherin in control and *ecHif2α*$^{-/-}$ EC. (Left panel) Quantification of VE-Cadherin intensity in control and *ecHif2α*$^{-/-}$ cells, control vs *ecHif2α*$^{-/-}$ p=0.0036, n=3-5 (F) Immunofluorescence staining of VE-Cadherin in primary Human Microvascular Endothelial Cells (HMVEC) transfected with or without si*Hif2α* and treated with 1% oxygen for overnight. The nuclei were stained Dapi (Blue), Ve-Cadherin (Red), Scale bar: 30 μm. (G) WB analysis of whole cell lysates from HMVEC transfected with or without scrambled or si*Hif2α* and treated with 1% oxygen for 16h. Quantification of VE-Cadherin protein levels (n=4) in lower panel. (H) Analysis of ECIS assays for *ecHif2α*$^{-/-}$ and wt EC cells. 90-100 % confluent monolayers of wt and *ecHif2α*$^{-/-}$ cells were cultured in collagen coated ECIS 8W10E+ arrays and treated with 1mM of DMOG to induce hypoxia. TER of cells was measured in Ohms using electric cell-substrate impedance sensing (ECIS) technology. Measurements were taken continuously at 3-minute intervals. (I) Analysis of endpoint normalized TER for ECIS assays. Results are shown as mean ± SEM for n=4 independent experiments. (J) ELISA measurement of plasma IL6 levels in MI induced *ecHif2α*$^{-/-}$ and control mice, n=3. Results are shown as mean ± SEM.

Figure 2: Worsened cardiac function and increased cardiac fibrosis associated with *Hif2α* deletion in cardiac endothelial cells after MI. (A) Control (*Hif2α*$^{flox/flox}$ with tamoxifen treatment) or *ecHif2α*$^{-/-}$ (*Hif2α*$^{flox/flox+CRE}$ with tamoxifen treatment) were subjected to MI for 7 or

28 days. Representative images of M-mode echocardiography in different groups as indicated at baseline and 28 days after MI. (B) Measurement of Ejection fraction (EF), and (C) Fractional shortening (FS) at baseline, 7 days and 28 days after MI induced controls and ecHif2a$^{-/-}$ mice. n=6 (D) Cardiac output. (E) Representative image of controls and *ecHif2α*$^{-/-}$ heart 28 days after MI. (F) Histological analysis of mouse heart sections stained by hematoxylin and eosin, and Masson trichrome 28 days after MI. (G-I) qPCR analysis of the mRNA levels for *Col13a1, Npr3* and *Bnp* in controls and *ecHif2α*$^{-/-}$ heart tissues. Data are presented as mean ± SEM., n = 3. (j) Kaplan–Meier survival curve in controls and *ecHif2α*$^{-/-}$ after MI, (n=34 ,WT:16, *ecHif2α*$^{-/-}$:18), p=0.05.

Figure 3: RNA-Seq analysis reveals altered gene expression in the mouse heart one month after MI. (A) Venn diagram showing the overlap of MI induced genes between controls and *ecHif2α*$^{-/-}$ heart tissues. (B) Volcano map of differentially expressed genes between controls and *ecHif2α*$^{-/-}$ heart tissues. Orange dots represent the upregulated genes and dark blue dots represent the downregulated genes. (C) Heatmap of differentially expressed genes in MI induced controls and *ecHif2α*$^{-/-}$ heart tissues, n=3. (D) KEEG pathway enrichment analysis of differentially expressed genes in controls and *ecHif2α*$^{-/-}$ samples shows dysregulation of multiple signaling pathways associated endothelial barrier function. (E-I) mRNA expression analysis of Plvap (E), P3h2 (F), Cdh5 (G), Il-6(H) and Vcam-1 (I) in controls and *ecHif2α*$^{-/-}$ samples after 28 days of MI. Data are presented as mean ± s.d., n = 3.

Figure 4: Loss of *Hif2α* Impairs Angiogenic Activity and Induces Cell Death in Endothelial Cells. (A) Representative images of HUVEC network, analyzed by the angiogenesis analyzer, Image J. Human umbilical vein endothelial cells (HUVEC) cells were plated on Matrigel pre-coated 24-well plates and transfected with either *Hif2α* siRNA or control-siRNA and exposed to normoxia and hypoxia (1% oxygen). Top panel of the image indicates meshes (blue), nodes (pink), junctions (yellow), and segment length (red). Bottom panel of the image shows capillary-like tube formation in 6 to 16h of seeding the cells. (B-E) Measurement of number of nodes (B), number of meshes (C), number of junctions (D) and total length (E), n=24. (F-H). Analysis of apoptosis in *Hif2α* knockdown HUVEC cells. HUVEC cells were transfected with either *Hif2α* siRNA or control siRNA and treated with or without 1% oxygen. Flow cytometric measurement of healthy cells (F), early-stage apoptotic cells (G) and late-stage apoptosis (H) based on 7-AAD labeling. Data analyzed using ordinary two-way ANOVA with Sidak's multiple comparisons test. n=4 or 5.

Figure 5: ARNT Overexpression Reverses Inflammatory Gene Expression and IL-6 Activity Induced by *Hif2α* Deletion Under Hypoxic Conditions. (A) WB analysis of ARNT, IL6, Hif2α and GAPDH in HAEC cells transfected with Hif2α siRNA and overexpressed with either EV or ARNT-oe and treated with 1% oxygen for 16h. (B) mRNA expression levels of *interleukin 6 (IL-6)*, *Intercellular adhesion molecule* (*ICAM), Vascular cell adhesion molecule 1 (VCAM-1)* and *TNFα* in controls and *ecHif2α*$^{-/-}$ heart tissue samples 28 days after MI, n=3. (C) Immunofluorescence staining of IL-6 in HAEC cells transfected with either *Hif2α* siRNA or scrambled siRNA and overexpressed with either EV or ARNT-oe and treated with 1% oxygen for 16h (D), quantification of IL-6 intensity. (E) WB analysis of ARNT, IL6, and GAPDH in HAEC cells transfected with Hif2α siRNA and overexpressed with either EV or ARNT-oe and treated with 1% oxygen for 16h.

Figure 6: **ARNT Overexpression Rescues Endothelial Barrier Dysfunction Induced by Hif2α Deletion Under Hypoxia in Human Cardiac Microvascular Endothelial Cells**. (A) Tunnel staining of HMVEC cells transfected with either siHif2α or scrambled siRNA and

overexpressed with ARNT-oe or Mutant-ARNT and treated with 1% oxygen for 16h, n=8. (B) Immunofluorescence staining of VE-Cadherin in Hif2α knockdown and ARNT-oe or ARNT-mutant overexpressing HMVEC cells, (n=3). (C-D) ECIS assays in HUVEC cells transfected with either Hif2α siRNA or control siRNA and treated with or without PBS (C) and DMOG (D), n=4. (E) ECIS assays in in HMVEC cells transfected with either siHif2α or scrambled siRNA and overexpressed with ARNT-oe or Mutant-ARNT and treated with DMOG for 16h, n=4.

Figure 7. **Hif2α/ARNT Heterodimers Directly Inhibit IL6 Transcription via DNA Binding**. Analysis of IL6 promoter activities in HEK293 cells. (A) Schematic diagram of IL-6 promoter reporter construct. (B) Normalized IL-6 promoter activities in HEK293 cells. Cells were transfected with human IL6 dual-reporter promoter clone and treated with or without 1% oxygen for 24, (n=4). (C) HEK293 cells were transfected with or without controls and *Hif2α* siRNA. After 24h human IL6 promoter containing dual-reporter vector were transfected and incubated for overnight. Cells were transfected with lentiviral vectors encoding either wild type ARNT (ARNT-WT) and a mutated form of ARNT (ARNT-Mut). Cells were treated with 1% oxygen for 24h before collecting the culture medium for analysis, (n=4, p=0.003). (D-E) ChIP-Qpcr analysis of IL6. HEK293 cells were treated with 1% oxygen or transfected with ARNT encoding lentivirus and treated with 1% oxygen. Chromatin immunoprecipitation was performed using the indicated antibodies. Data are presented as mean ± s.d., n= 6. (F) Diagram of Mechanism of Hif2α/ARNT-mediated regulation of cardiac endothelial barrier function and cardiac function during myocardial infarction.

Author Contributions

The study was designed and the manuscript was written by KU and RW. KU and LA conducted the experiments with assistance from QZ, LL, KP, ZH, and AS. Bioinformatics analysis was performed by YL. Animal surgery was carried out by RW, who also supervised the research. QS, QZ, WS, YF, DW, and JL provided suggestions and consulting on the research and contributed to the writing of the manuscript. All authors have read and approved the final version.

Funding Information

RW was supported by the 1R01HL140114-01A1, Chicago DRTC (NIH/P30 DK020595), and CTSA-ITM Core subsidies funding (through NIH UL1 TR000430).

Acknowledgments:

Inducible VE-cadherin-CreERT2 mice were provided by JK Liao. Sperm was a gift from Dr. Yoshiaki Kubota (Keio University, Tokyo, Japan) to JK Liao. Lentiviral vectors for expression of ARNT, mutant ARNT, or a scramble control were packaged and titrated by the Northwestern Genomic Editing and Screening Core (GET iN Core) under the supervision of Dr. Pankaj Bhalla. We also want to thank The University of Chicago Human Tissue Resource Center (RRID:SCR_019199), especially Terri Shihong Li, for their assistance with tissue staining. Figure 7F was created with BioRender.com.

Conflict of Interest

The authors declare no competing financial interests.

References

1. Khan MA, Hashim MJ, Mustafa H, Baniyas MY, Al Suwaidi S, AlKatheeri R, Alblooshi FMK, Almatrooshi M, Alzaabi MEH, Al Darmaki RS and Lootah S. Global Epidemiology of Ischemic Heart Disease: Results from the Global Burden of Disease Study. *Cureus*. 2020;12:e9349.
2. Eltzschig HK and Eckle T. Ischemia and reperfusion--from mechanism to translation. *Nat Med*. 2011;17:1391-401.
3. Dongaonkar RM, Stewart RH, Geissler HJ and Laine GA. Myocardial microvascular permeability, interstitial oedema, and compromised cardiac function. *Cardiovasc Res*. 2010;87:331-9.
4. Zhang H, Kim H, Park BW, Noh M, Kim Y, Park J, Park JH, Kim JJ, Sim WS, Ban K, Park HJ and Kwon YG. CU06-1004 enhances vascular integrity and improves cardiac remodeling by suppressing edema and inflammation in myocardial ischemia-reperfusion injury. *Experimental & molecular medicine*. 2022;54:23-34.
5. Koeppen M, Lee JW, Seo SW, Brodsky KS, Kreth S, Yang IV, Buttrick PM, Eckle T and Eltzschig HK. Hypoxia-inducible factor 2-alpha-dependent induction of amphiregulin dampens myocardial ischemia-reperfusion injury. *Nat Commun*. 2018;9:816.
6. Nguyen T, Zheng M, Knapp M, Sladojevic N, Zhang Q, Ai L, Harrison D, Chen A, Sitikov A, Shen L, Gonzalez FJ, Zhao Q, Fang Y, Liao JJK and Wu R. Endothelial Aryl Hydrocarbon Receptor Nuclear Translocator Mediates the Angiogenic Response to Peripheral Ischemia in Mice With Type 2 Diabetes Mellitus. *Front Cell Dev Biol*. 2021;9:691801.
7. Ullah K and Wu R. Hypoxia-Inducible Factor Regulates Endothelial Metabolism in Cardiovascular Disease. *Front Physiol*. 2021;12:670653.
8. Maltepe E, Schmidt JV, Baunoch D, Bradfield CA and Simon MC. Abnormal angiogenesis and responses to glucose and oxygen deprivation in mice lacking the protein ARNT. *Nature*. 1997;386:403-7.
9. Tekin D, Dursun AD and Xi L. Hypoxia inducible factor 1 (HIF-1) and cardioprotection. *Acta Pharmacol Sin*. 2010;31:1085-94.
10. Sarkar K, Cai Z, Gupta R, Parajuli N, Fox-Talbot K, Darshan MS, Gonzalez FJ and Semenza GL. Hypoxia-inducible factor 1 transcriptional activity in endothelial cells is required for acute phase cardioprotection induced by ischemic preconditioning. *Proc Natl Acad Sci U S A*. 2012;109:10504-9.
11. Zheng J, Chen P, Zhong J, Cheng Y, Chen H, He Y and Chen C. HIF1alpha in myocardial ischemiareperfusion injury (Review). *Mol Med Rep*. 2021;23.
12. Wiesener MS, Jurgensen JS, Rosenberger C, Scholze CK, Horstrup JH, Warnecke C, Mandriota S, Bechmann I, Frei UA, Pugh CW, Ratcliffe PJ, Bachmann S, Maxwell PH and Eckardt KU. Widespread hypoxia-inducible expression of HIF-2alpha in distinct cell populations of different organs. *FASEB J*. 2003;17:271-3.
13. Dai Z, Zhu MM, Peng Y, Machireddy N, Evans CE, Machado R, Zhang X and Zhao YY. Therapeutic Targeting of Vascular Remodeling and Right Heart Failure in Pulmonary Arterial Hypertension with a HIF-2alpha Inhibitor. *American journal of respiratory and critical care medicine*. 2018;198:1423-1434.
14. Skuli N, Liu L, Runge A, Wang T, Yuan L, Patel S, Iruela-Arispe L, Simon MC and Keith B. Endothelial deletion of hypoxia-inducible factor-2alpha (HIF-2alpha) alters vascular function and tumor angiogenesis. *Blood*. 2009;114:469-77.
15. Dunwoodie SL. The role of hypoxia in development of the Mammalian embryo. *Dev Cell*. 2009;17:755-73.

16. Licht AH, Muller-Holtkamp F, Flamme I and Breier G. Inhibition of hypoxia-inducible factor activity in endothelial cells disrupts embryonic cardiovascular development. *Blood*. 2006;107:584-90.
17. Gong H, Rehman J, Tang H, Wary K, Mittal M, Chaturvedi P, Zhao YY, Komarova YA, Vogel SM and Malik AB. Corrigendum. HIF2alpha signaling inhibits adherens junctional disruption in acute lung injury. *The Journal of clinical investigation*. 2015;125:1364.
18. Alva JA, Zovein AC, Monvoisin A, Murphy T, Salazar A, Harvey NL, Carmeliet P and Iruela-Arispe ML. VE-Cadherin-Cre-recombinase transgenic mouse: a tool for lineage analysis and gene deletion in endothelial cells. *Dev Dyn*. 2006;235:759-67.
19. Fahey E and Doyle SL. IL-1 Family Cytokine Regulation of Vascular Permeability and Angiogenesis. *Front Immunol*. 2019;10:1426.
20. Khurana R, Simons M, Martin JF and Zachary IC. Role of angiogenesis in cardiovascular disease: a critical appraisal. *Circulation*. 2005;112:1813-24.
21. Bourner LA, Muro I, Cooper AM, Choudhury BK, Bailey AO, Russell WK, Khanipov K, Golovko G and Wright CW. AhR promotes phosphorylation of ARNT isoform 1 in human T cell malignancies as a switch for optimal AhR activity. *Proceedings of the National Academy of Sciences of the United States of America*. 2022;119.
22. Bautista L, Castro MJ, Lopez-Barneo J and Castellano A. Hypoxia inducible factor-2alpha stabilization and maxi-K+ channel beta1-subunit gene repression by hypoxia in cardiac myocytes: role in preconditioning. *Circ Res*. 2009;104:1364-72.
23. Eckle T, Kohler D, Lehmann R, El Kasmi K and Eltzschig HK. Hypoxia-inducible factor-1 is central to cardioprotection: a new paradigm for ischemic preconditioning. *Circulation*. 2008;118:166-75.
24. Du X, Yang J, Liu C, Wang S, Zhang C, Zhao H, Du H and Geng X. Hypoxia-Inducible Factor 1alpha and 2alpha Have Beneficial Effects in Remote Ischemic Preconditioning Against Stroke by Modulating Inflammatory Responses in Aged Rats. *Front Aging Neurosci*. 2020;12:54.
25. Kapitsinou PP, Sano H, Michael M, Kobayashi H, Davidoff O, Bian A, Yao B, Zhang MZ, Harris RC, Duffy KJ, Erickson-Miller CL, Sutton TA and Haase VH. Endothelial HIF-2 mediates protection and recovery from ischemic kidney injury. *The Journal of clinical investigation*. 2014;124:2396-409.
26. van der Wijk AE, Wisniewska-Kruk J, Vogels IMC, van Veen HA, Ip WF, van der Wel NN, van Noorden CJF, Schlingemann RO and Klaassen I. Expression patterns of endothelial permeability pathways in the development of the blood-retinal barrier in mice. *FASEB J*. 2019;33:5320-5333.
27. Vestweber D. VE-cadherin: the major endothelial adhesion molecule controlling cellular junctions and blood vessel formation. *Arterioscler Thromb Vasc Biol*. 2008;28:223-32.
28. Abelanet A, Camoin M, Rubin S, Bougaran P, Delobel V, Pernot M, Forfar I, Guilbeau-Frugier C, Gales C, Bats ML, Renault MA, Dufourcq P, Couffinhal T and Duplaa C. Increased Capillary Permeability in Heart Induces Diastolic Dysfunction Independently of Inflammation, Fibrosis, or Cardiomyocyte Dysfunction. *Arterioscler Thromb Vasc Biol*. 2022;42:745-763.
29. van den Oever IA, Raterman HG, Nurmohamed MT and Simsek S. Endothelial dysfunction, inflammation, and apoptosis in diabetes mellitus. *Mediators Inflamm*. 2010;2010:792393.

30. Su J, An XR, Li Q, Li XX, Cong XD and Xu M. Improvement of vascular dysfunction by argirein through inhibiting endothelial cell apoptosis associated with ET-1/Nox4 signal pathway in diabetic rats. *Sci Rep*. 2018;8:12620.
31. Claesson-Welsh L, Dejana E and McDonald DM. Permeability of the Endothelial Barrier: Identifying and Reconciling Controversies. *Trends Mol Med*. 2021;27:314-331.
32. Ungvari Z, Tarantini S, Kiss T, Wren JD, Giles CB, Griffin CT, Murfee WL, Pacher P and Csiszar A. Endothelial dysfunction and angiogenesis impairment in the ageing vasculature. *Nat Rev Cardiol*. 2018;15:555-565.
33. Spyridopoulos I, Luedemann C, Chen D, Kearney M, Chen D, Murohara T, Principe N, Isner JM and Losordo DW. Divergence of angiogenic and vascular permeability signaling by VEGF: inhibition of protein kinase C suppresses VEGF-induced angiogenesis, but promotes VEGF-induced, NO-dependent vascular permeability. *Arterioscler Thromb Vasc Biol*. 2002;22:901-6.
34. Watts ER and Walmsley SR. Inflammation and Hypoxia: HIF and PHD Isoform Selectivity. *Trends Mol Med*. 2019;25:33-46.
35. Meneses AM and Wielockx B. PHD2: from hypoxia regulation to disease progression. *Hypoxia (Auckl)*. 2016;4:53-67.
36. Rajendran G, Schonfeld MP, Tiwari R, Huang S, Torosyan R, Fields T, Park J, Susztak K and Kapitsinou PP. Inhibition of Endothelial PHD2 Suppresses Post-Ischemic Kidney Inflammation through Hypoxia-Inducible Factor-1. *J Am Soc Nephrol*. 2020;31:501-516.
37. Castellon X and Bogdanova V. Chronic Inflammatory Diseases and Endothelial Dysfunction. *Aging Dis*. 2016;7:81-9.
38. Chistiakov DA, Orekhov AN and Bobryshev YV. Endothelial Barrier and Its Abnormalities in Cardiovascular Disease. *Front Physiol*. 2015;6:365.
39. He K, Chen X, Han C, Xu L, Zhang J, Zhang M and Xia Q. Lipopolysaccharide-induced cross-tolerance against renal ischemia-reperfusion injury is mediated by hypoxia-inducible factor-2alpha-regulated nitric oxide production. *Kidney Int*. 2014;85:276-88.
40. Gong H, Rehman J, Tang H, Wary K, Mittal M, Chaturvedi P, Zhao YY, Komarova YA, Vogel SM and Malik AB. HIF2alpha signaling inhibits adherens junctional disruption in acute lung injury. *The Journal of clinical investigation*. 2015;125:652-64.
41. Yang YC, Fu H, Zhang B and Wu YB. Interleukin-6 Downregulates the Expression of Vascular Endothelial-Cadherin and Increases Permeability in Renal Glomerular Endothelial Cells via the Trans-Signaling Pathway. *Inflammation*. 2022;45:2544-2558.
42. Alsaffar H, Martino N, Garrett JP and Adam AP. Interleukin-6 promotes a sustained loss of endothelial barrier function via Janus kinase-mediated STAT3 phosphorylation and de novo protein synthesis. *Am J Physiol Cell Physiol*. 2018;314:C589-C602.
43. Valle ML, Dworshak J, Sharma A, Ibrahim AS, Al-Shabrawey M and Sharma S. Inhibition of interleukin-6 trans-signaling prevents inflammation and endothelial barrier disruption in retinal endothelial cells. *Exp Eye Res*. 2019;178:27-36.
44. Imtiyaz HZ, Williams EP, Hickey MM, Patel SA, Durham AC, Yuan LJ, Hammond R, Gimotty PA, Keith B and Simon MC. Hypoxia-inducible factor 2alpha regulates macrophage function in mouse models of acute and tumor inflammation. *J Clin Invest*. 2010;120:2699-714.
45. Wu JW, Hu H, Li D and Ma LK. Hypoxia-inducible factor 2-alpha-dependent induction of IL-6 protects the heart from ischemia/reperfusion injury. *Aging (Albany NY)*. 2021;13:3443-3458.

46. Jiang X, Tian W, Granucci EJ, Tu AB, Kim D, Dahms P, Pasupneti S, Peng G, Kim Y, Lim AH, Espinoza FH, Cribb M, Dixon JB, Rockson SG, Semenza GL and Nicolls MR. Decreased lymphatic HIF-2alpha accentuates lymphatic remodeling in lymphedema. *J Clin Invest*. 2020;130:5562-5575.
47. Fan Q, Mao H, Xie L and Pi X. Prolyl Hydroxylase Domain-2 Protein Regulates Lipopolysaccharide-Induced Vascular Inflammation. *Am J Pathol*. 2019;189:200-213.
48. Macias D, Moore S, Crosby A, Southwood M, Du X, Tan H, Xie S, Vassallo A, Wood AJT, Wallace EM and Cowburn AS. Targeting HIF2alpha-ARNT hetero-dimerisation as a novel therapeutic strategy for pulmonary arterial hypertension. *Eur Respir J*. 2021;57.
49. Yim SH, Shah Y, Tomita S, Morris HD, Gavrilova O, Lambert G, Ward JM and Gonzalez FJ. Disruption of the Arnt gene in endothelial cells causes hepatic vascular defects and partial embryonic lethality in mice. *Hepatology*. 2006;44:550-60.
50. Lee KY, Gesta S, Boucher J, Wang XL and Kahn CR. The differential role of Hif1beta/Arnt and the hypoxic response in adipose function, fibrosis, and inflammation. *Cell Metab*. 2011;14:491-503.

Figure 1

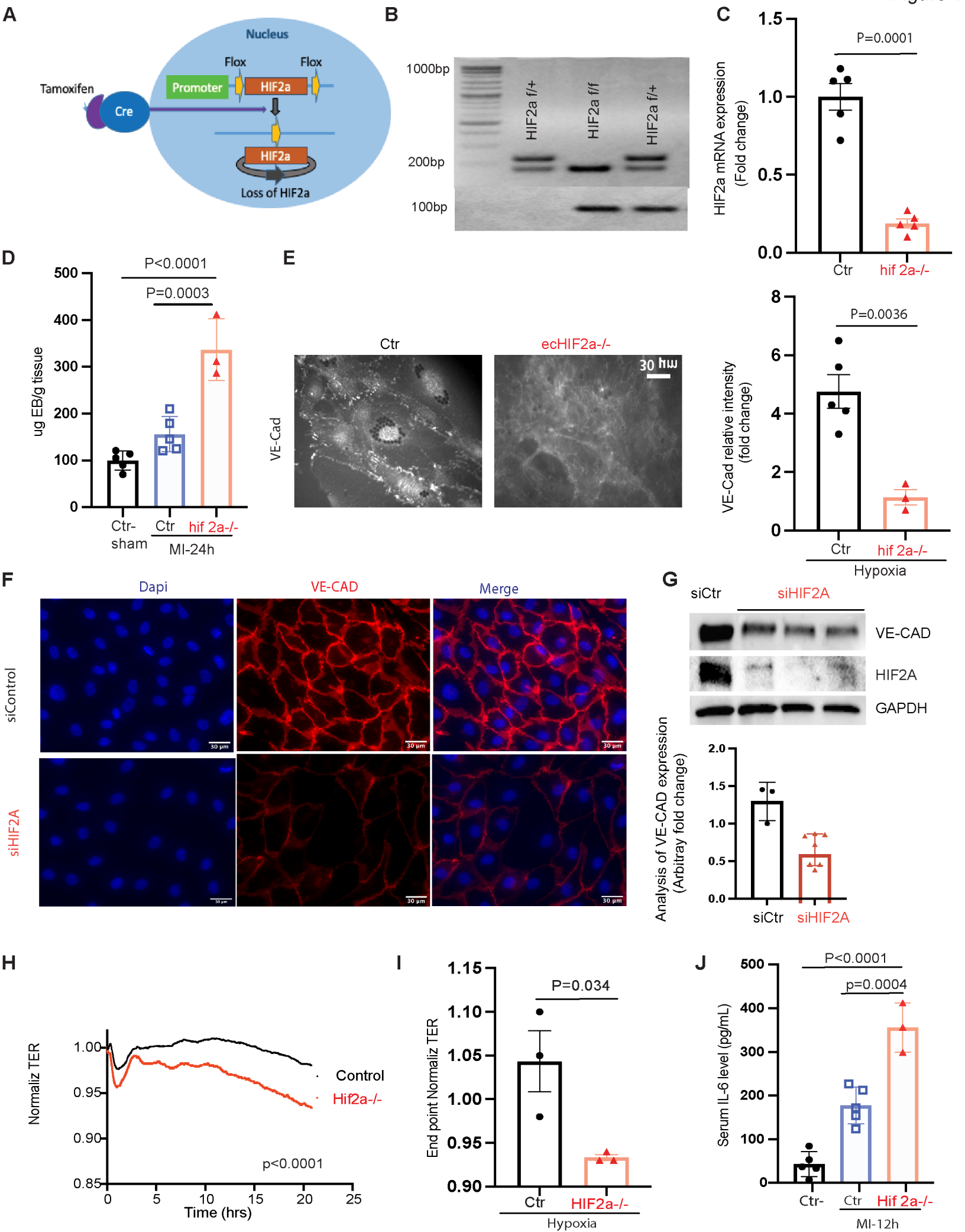
A
Nucleus
Flox
Flox
Tamoxifen
Promoter
HIF2a
Cre
HIF2a
Loss of HIF2a
B
1000bp
200bp
100bp
HIF2a f/+
HIF2a f/f
HIF2a f/+
C
P=0.0001
HIF2a mRNA expression (Fold change)
Ctr
hif 2a-/-
D
P<0.0001
P=0.0003
ug EB/g tissue
Ctr-sham
Ctr
hif 2a-/-
MI-24h
E
Ctr
ecHIF2a-/-
VE-Cad
30 µm
VE-Cad relative intensity (fold change)
P=0.0036
Ctr
hif 2a-/-
Hypoxia
F
Dapi
VE-CAD
Merge
siControl
siHIF2A
G
siCtr
siHIF2A
VE-CAD
HIF2A
GAPDH
Analysis of VE-CAD expression (Arbitray fold change)
siCtr
siHIF2A
H
Normaliz TER
Control
Hif2a-/-
p<0.0001
Time (hrs)
I
P=0.034
End point Normaliz TER
Ctr
HIF2a-/-
Hypoxia
J
P<0.0001
p=0.0004
Serum IL-6 level (pg/mL)
Ctr-
Ctr
Hif 2a-/-
MI-12h

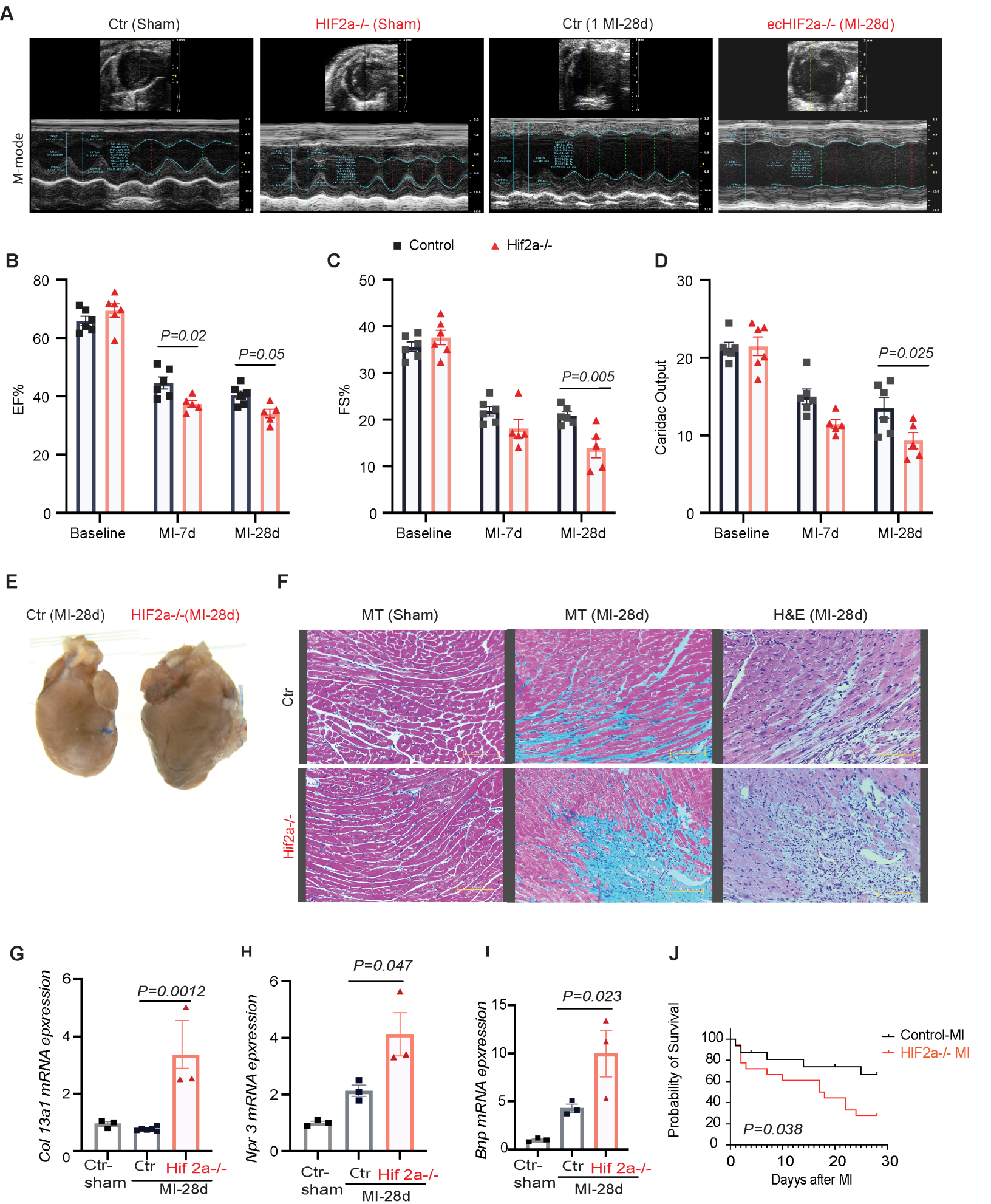
A
Ctr (Sham)
HIF2a-/- (Sham)
Ctr (1 MI-28d)
ecHIF2a-/- (MI-28d)
M-mode
Control
Hif2a-/-
B
EF%
P=0.02
P=0.05
Baseline
MI-7d
MI-28d
C
FS%
P=0.005
D
Caridac Output
P=0.025
E
Ctr (MI-28d)
HIF2a-/-(MI-28d)
F
MT (Sham)
MT (MI-28d)
H&E (MI-28d)
Ctr
Hif2a-/-
G
Col 13a1 mRNA epxression
P=0.0012
Ctr-sham
Ctr
Hif 2a-/-
MI-28d
H
Npr 3 mRNA epxression
P=0.047
I
Bnp mRNA epxression
P=0.023
J
Probability of Survival
Control-MI
HIF2a-/- MI
P=0.038
Dayys after MI

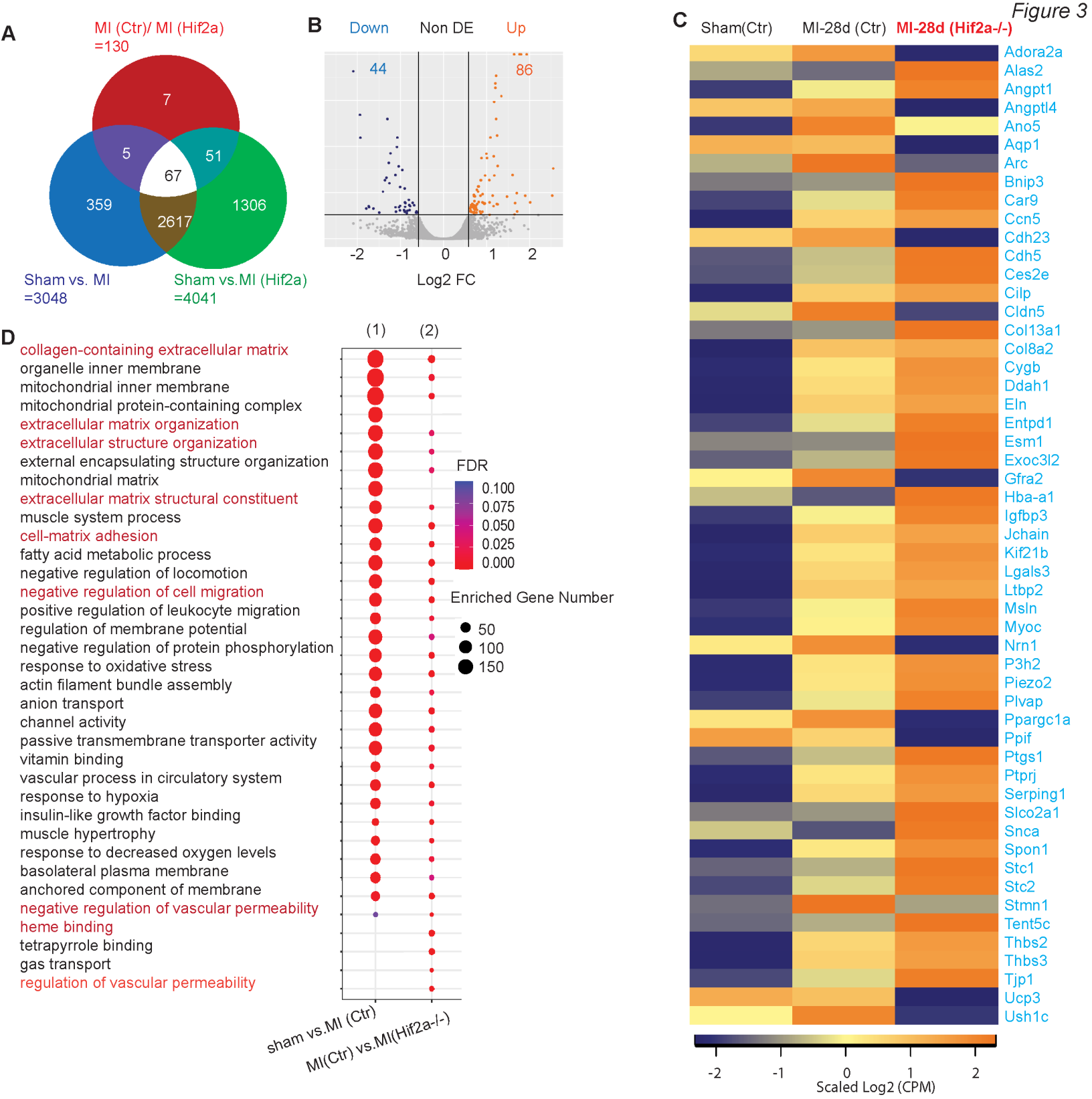
A
MI (Ctr)/ MI (Hif2a) =130
7
5
51
67
359
2617
1306
Sham vs. MI =3048
Sham vs.MI (Hif2a) =4041
B
Down
Non DE
Up
44
86
-2
-1
0
1
2
Log2 FC
C
Sham(Ctr)
MI-28d (Ctr)
MI-28d (Hif2a-/-)
Adora2a
Alas2
Angpt1
Angptl4
Ano5
Aqp1
Arc
Bnip3
Car9
Ccn5
Cdh23
Cdh5
Ces2e
Cilp
Cldn5
Col13a1
Col8a2
Cygb
Ddah1
Eln
Entpd1
Esm1
Exoc3l2
Gfra2
Hba-a1
Igfbp3
Jchain
Kif21b
Lgals3
Ltbp2
Msln
Myoc
Nrn1
P3h2
Piezo2
Plvap
Ppargc1a
Ppif
Ptgs1
Ptprj
Serping1
Slco2a1
Snca
Spon1
Stc1
Stc2
Stmn1
Tent5c
Thbs2
Thbs3
Tjp1
Ucp3
Ush1c
-2
-1
0
1
2
Scaled Log2 (CPM)
D
(1)
(2)
collagen-containing extracellular matrix
organelle inner membrane
mitochondrial inner membrane
mitochondrial protein-containing complex
extracellular matrix organization
extracellular structure organization
external encapsulating structure organization
mitochondrial matrix
extracellular matrix structural constituent
muscle system process
cell-matrix adhesion
fatty acid metabolic process
negative regulation of locomotion
negative regulation of cell migration
positive regulation of leukocyte migration
regulation of membrane potential
negative regulation of protein phosphorylation
response to oxidative stress
actin filament bundle assembly
anion transport
channel activity
passive transmembrane transporter activity
vitamin binding
vascular process in circulatory system
response to hypoxia
insulin-like growth factor binding
muscle hypertrophy
response to decreased oxygen levels
basolateral plasma membrane
anchored component of membrane
negative regulation of vascular permeability
heme binding
tetrapyrrole binding
gas transport
regulation of vascular permeability
FDR
0.100
0.075
0.050
0.025
0.000
Enriched Gene Number
50
100
150
sham vs.MI (Ctr)
MI(Ctr) vs.MI(Hif2a-/-)
E
Plvap mRNA epxression
P<0.0001
P<0.0001
Ctr-sham
Ctr
Hif 2a-/-
MI-28d
F
P3h2 mRNA epxression
P<0.0001
P<0.0001
Ctr-sham
Ctr
Hif 2a-/-
MI-28d
G
Cdh5 mRNA epxression
P=0.0009
P=0.0032
Ctr-sham
Ctr
Hif 2a-/-
MI-28d
H
IL-6 mRNA epxression
p=0.01
p=0.035
Ctr-sham
Ctr
Hif2a-/-
MI-28d
I
VCAM-1 mRNA epxression
p<0.0001
p=0.002
Ctr-sham
Ctr
Hif2a-/-
MI

Figure 4

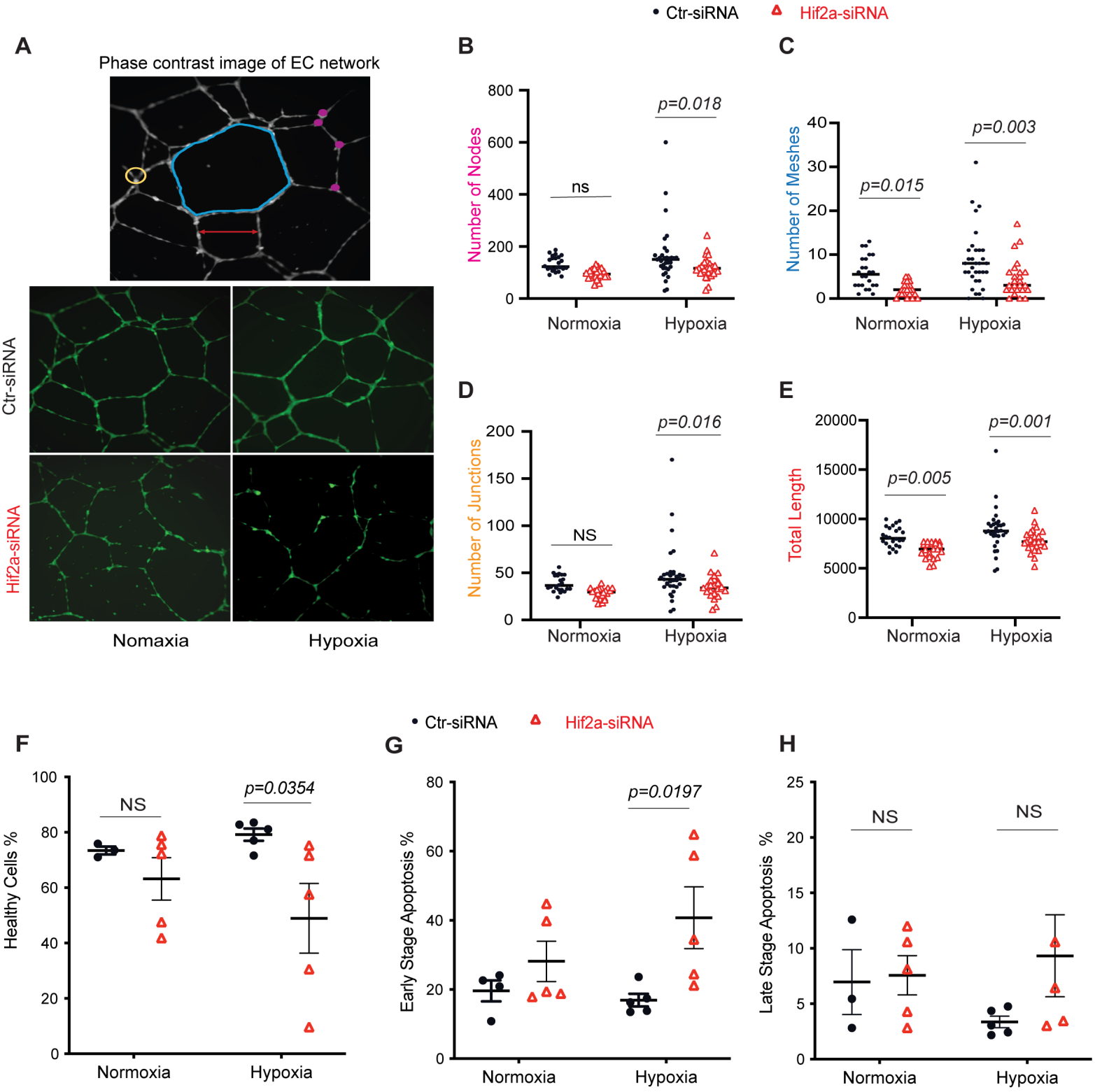
A
Phase contrast image of EC network
Ctr-siRNA
Hif2a-siRNA
Nomaxia
Hypoxia
• Ctr-siRNA
Hif2a-siRNA
B
Number of Nodes
ns
p=0.018
Normoxia
Hypoxia
C
Number of Meshes
p=0.015
p=0.003
Normoxia
Hypoxia
D
Number of Junctions
NS
p=0.016
Normoxia
Hypoxia
E
Total Length
p=0.005
p=0.001
Normoxia
Hypoxia
• Ctr-siRNA
Hif2a-siRNA
F
Healthy Cells %
NS
p=0.0354
Normoxia
Hypoxia
G
Early Stage Apoptosis %
p=0.0197
Normoxia
Hypoxia
H
Late Stage Apoptosis %
NS
NS
Normoxia
Hypoxia

Figure 5

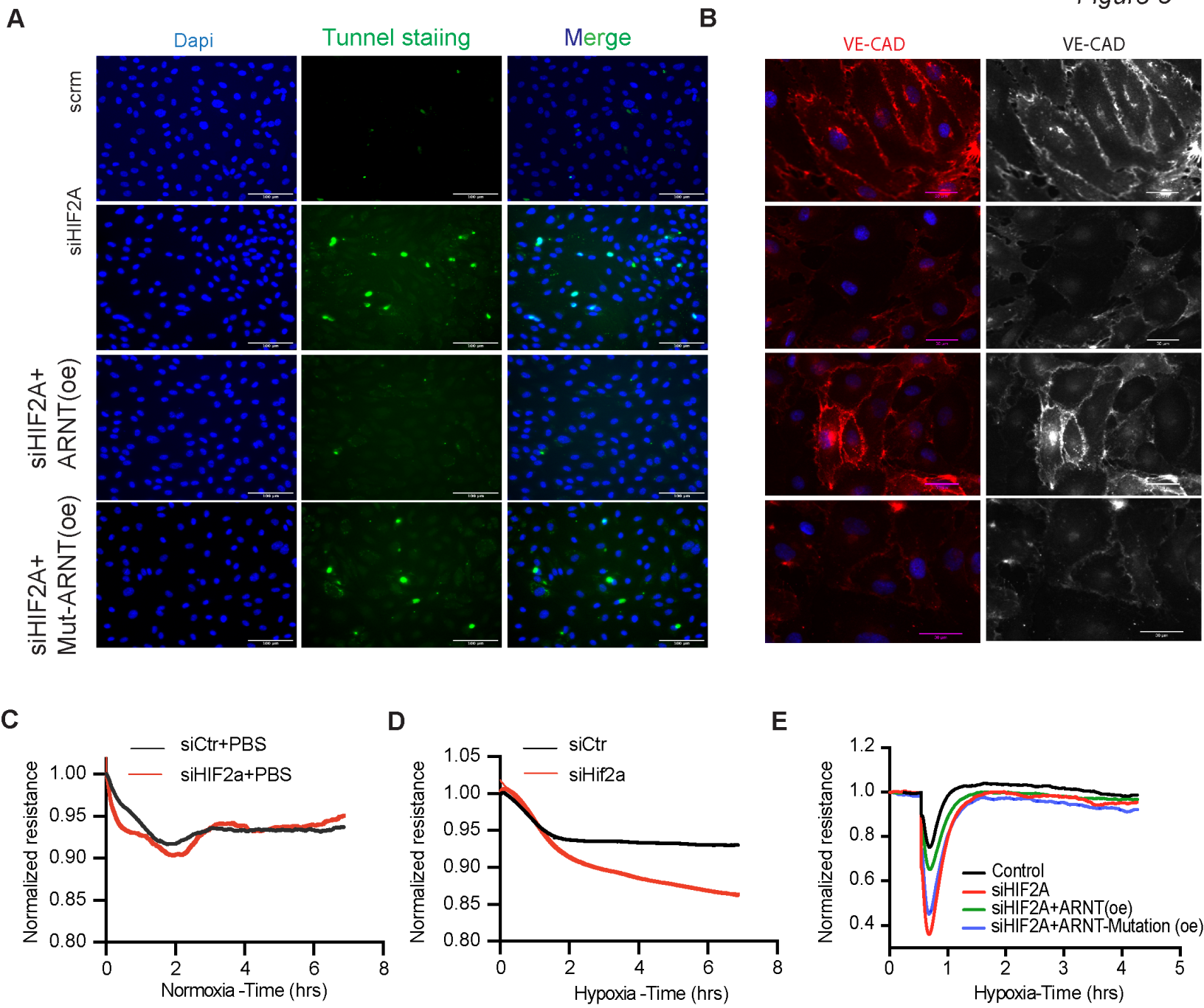
A
Dapi
Tunnel staiing
Merge
scrm
siHIF2A
siHIF2A+ ARNT(oe)
siHIF2A+ Mut-ARNT(oe)
B
VE-CAD
VE-CAD
C
siCtr+PBS
siHIF2a+PBS
Normalized resistance
Normoxia -Time (hrs)
D
siCtr
siHif2a
Normalized resistance
Hypoxia -Time (hrs)
E
Control
siHIF2A
siHIF2A+ARNT(oe)
siHIF2A+ARNT-Mutation (oe)
Normalized resistance
Hypoxia-Time (hrs)

Figure 6

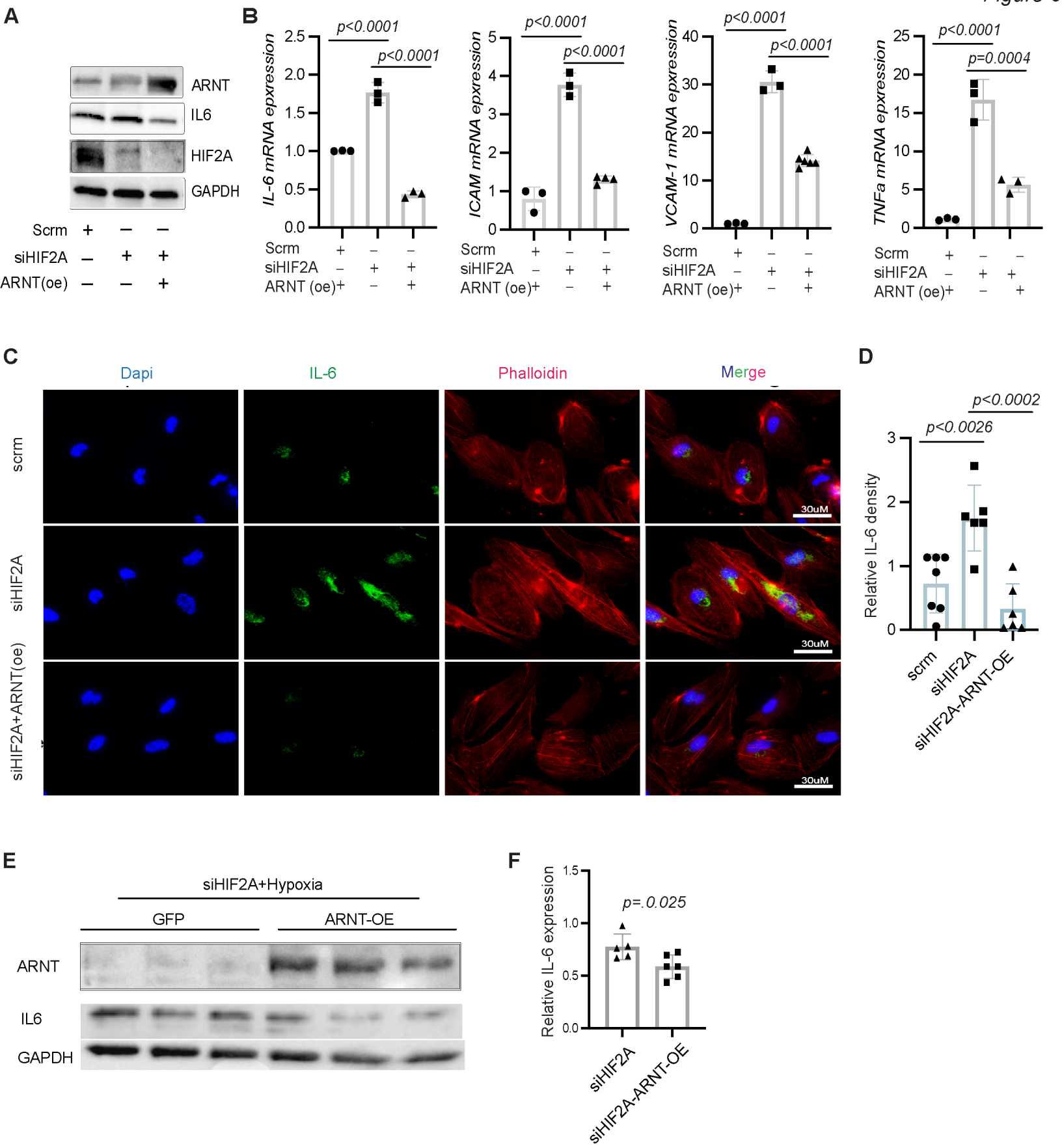
A
ARNT
IL6
HIF2A
GAPDH
Scrm + – –
siHIF2A – + +
ARNT(oe) – – +
B
IL-6 mRNA epxression
ICAM mRNA epxression
VCAM-1 mRNA epxression
TNFa mRNA epxression
p<0.0001
p=0.0004
Scrm + – –
siHIF2A – + +
ARNT (oe)+ – +
C
Dapi
IL-6
Phalloidin
Merge
scrm
siHIF2A
siHIF2A+ARNT(oe)
30uM
D
Relative IL-6 density
p<0.0026
p<0.0002
scrm
siHIF2A
siHIF2A-ARNT-OE
E
siHIF2A+Hypoxia
GFP
ARNT-OE
ARNT
IL6
GAPDH
F
Relative IL-6 expression
p=.0.025
siHIF2A
siHIF2A-ARNT-OE

Figure 7

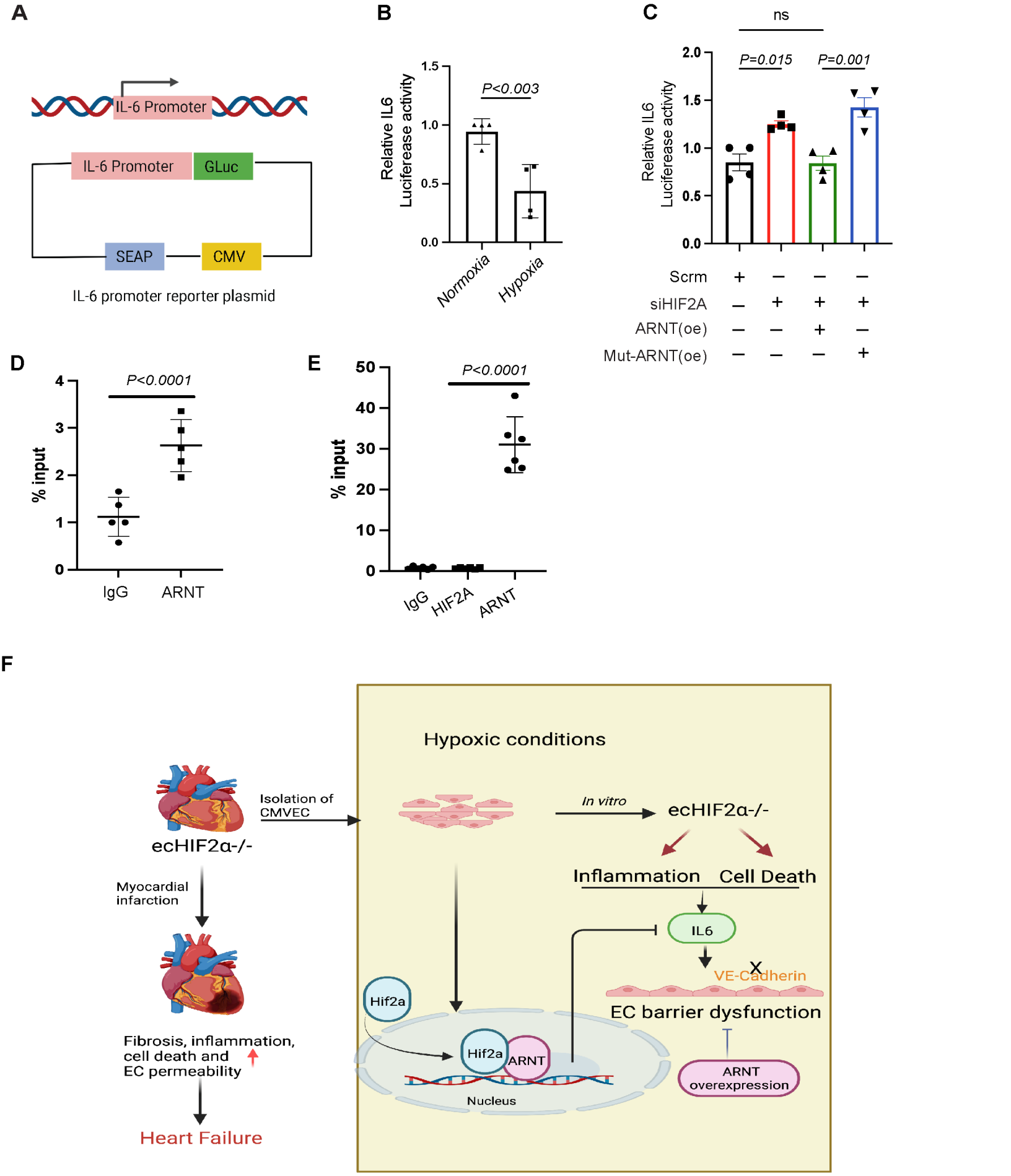
A
IL-6 Promoter
IL-6 Promoter
GLuc
SEAP
CMV
IL-6 promoter reporter plasmid
B
Relative IL6 Luciferease activity
P<0.003
Normoxia
Hypoxia
C
ns
P=0.015
P=0.001
Relative IL6 Luciferease activity
Scrm
siHIF2A
ARNT(oe)
Mut-ARNT(oe)
D
P<0.0001
% input
IgG
ARNT
E
P<0.0001
% input
IgG
HIF2A
ARNT
F
Isolation of CMVEC
ecHIF2α-/-
Myocardial infarction
Fibrosis, inflammation, cell death and EC permeability
Heart Failure
Hypoxic conditions
In vitro
ecHIF2α-/-
Inflammation
Cell Death
IL6
VE-Cadherin
EC barrier dysfunction
Hif2a
Hif2a
ARNT
Nucleus
ARNT overexpression